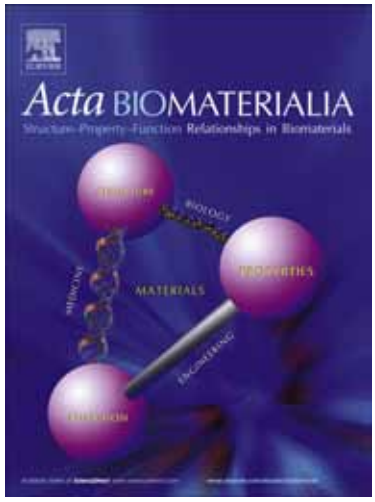


# Electrospun Conductive Nanofibrous Scaffolds for Engineering Cardiac Tissue and 3D Bioactuators

Ling Wang, Yaobin Wu, Tianli Hu, Baolin Guo, Peter X. Ma

PII: S1742-7061(17)30418-X
DOI: http://dx.doi.org/10.1016/j.actbio.2017.06.036
Reference: ACTBIO 4957

To appear in: *Acta Biomaterialia*

Received Date: 15 March 2017
Revised Date: 25 May 2017
Accepted Date: 26 June 2017

Please cite this article as: Wang, L., Wu, Y., Hu, T., Guo, B., Ma, P.X., Electrospun Conductive Nanofibrous Scaffolds for Engineering Cardiac Tissue and 3D Bioactuators, *Acta Biomaterialia* (2017), doi: http://dx.doi.org/10.1016/j.actbio.2017.06.036

# Electrospun Conductive Nanofibrous Scaffolds for Engineering Cardiac Tissue and 3D Bioactuators

Ling Wang [a], Yaobin Wu [a], Tianli Hu [a], Baolin Guo [a,*], Peter X Ma [a, b,c,d,e,*]

[a] *Frontier Institute of Science and Technology, and State Key Laboratory for Mechanical Behavior of Materials, Xi'an Jiaotong University, Xi'an, 710049, China*

[b] *Department of Biomedical Engineering, University of Michigan, Ann Arbor, MI 48109, USA*

[c] *Department of Biologic and Materials Sciences, University of Michigan, Ann Arbor, MI 48109, USA*

[d] *Macromolecular Science and Engineering Center, University of Michigan, Ann Arbor, MI 48109, USA*

[e] *Department of Materials Science and Engineering, University of Michigan, Ann Arbor, MI 48109, USA*

* To whom correspondence should be addressed. Tel.:+86-29-83395361. Fax: +86-29-83395131. E-mail: baoling@mail.xjtu.edu.cn, mapx@umich.edu.

**Abstract:** Mimicking the nanofibrous structure similar to extracellular matrix and conductivity for electrical propagation of native myocardium would be highly beneficial for cardiac tissue engineering and cardiomyocytes-based bioactuators. Herein, we developed conductive nanofibrous sheets with electrical conductivity and nanofibrous structure composed of poly(L-lactic acid) (PLA) blending with polyaniline (PANI) for cardiac tissue engineering and cardiomyocytes-based 3D bioactuators. Incorporating of varying contents of PANI from 0 wt% to 3 wt% into the PLA polymer, the electrospun nanofibrous sheets showed enhanced conductivity while maintaining the same fiber diameter. These PLA/PANI conductive nanofibrous sheets exhibited good cell viability and promoting effect on differentiation of H9c2 cardiomyoblasts in terms of maturation index and fusion index. Moreover, PLA/PANI nanofibrous sheets enhanced the cell-cell interaction, maturation and spontaneous beating of primary cardiomyocytes. Furthermore, the cardiomyocytes-laden PLA/PANI conductive nanofibrous sheets can form 3D bioactuators with tubular and folding shapes, and spontaneously beat with much higher frequency and displacement than that on cardiomyocytes-laden PLA nanofibrous sheets. Therefore, these PLA/PANI conductive nanofibrous sheets with conductivity and extracellular matrix like nanostructure demonstrated promising potential in cardiac tissue engineering and cardiomyocytes-based 3D bioactuators.

**Keywords:** cardiac tissue engineering; bioactuators; cardiomyocytes; conductive nanofibrous sheets; polyaniline

## 1 Introduction

Cardiac diseases and heart failure are effecting numerous patients around the world in the past two decades, and myocardial infarction is the major cause of death worldwide.[1, 2] The regeneration of damaged heart tissue is severely limited by the poor regenerative potential of myocardium and the scar formation around the infarction sites.[3, 4] Tissue engineering is a promising approach for cardiac regeneration by combining biomaterials and cardiomyocytes (CMs) to generate engineered cardiac tissue constructs, and also has potential application for fabricating CMs-based bioactuators.[5-13] Over the past decade, bioactuators have been especially studied due to the exploitation of self-actuating behavior of living cells for engineering biological machines and other applications.[14-17] For instance, many kinds of living cells such as skeletal muscle cells have been used to combine with biomaterial scaffolds to develop various bioactuators including engineered nanomembranes and biological machines.[18-20] Particularly, bioactuators based on CMs have been so far paid more attention due to their spontaneous motion by integrating the spontaneous beating behavior of CMs into various polymer structures.[15, 21, 22] Specially, many reports have focused on utilizing poly(dimethylsiloxane) (PDMS) as fundamental material to create CMs-based bioactuators.[15, 23] Although PDMS could be easily fabricated with different modulus and structures, the lack of bioactivities and non-biodegradability of these PDMS-based materials limited their clinical use in vivo. On the other hand, polymer structures that can mimic the extracellular matrix (ECM) of myocardium would be

highly beneficial, because the ECM of myocardium plays a critical role in providing nanofibrous microenvironment for cardiac cell adhesion, maturation and function.[24-26] Unfortunately, PDMS was difficult to be prepared into nanofibrous structures mimicking the ECM of myocardium, which is another great barrier for its practical applications. Therefore, considering the complex microstructure of myocardium, it remains an ongoing challenge to prepare biomimetic cardiac substitutes and develop functional CM-based bioactuators.

Many techniques have been recently developed to fabricate various polymer structures containing nanofibrous architecture for mimicking the ECM of myocardium.[24, 27-30] Among these approaches, electrospinning has been regarded as a simple and versatile method to prepare nanofibrous scaffolds, and also allowed for the manipulation of many parameters, including fiber diameter, fiber orientation and fiber density.[31-37] Due to the similarity between nanofibrous structure and ECM of myocardium, electrospun nanofibrous scaffold provides sufficient support for cardiac cells.[27-29] Moreover, CMs are electroactive cells and can be spontaneously contractile under electric signal propagation.[38, 39] Therefore, to mimic the native myocardium, the biomaterials should not only possess ECM-liked nanofibrous structure, but also exhibit conductive property to promote electrical propagation for functional coupling of CMs. However, there are still challenges for fabricating such suitable biomaterials for cardiac tissue engineering and CMs-based bioactuators.

To address these challenges, many studies have focused on developing electrically conductive nanofibrous scaffolds through incorporation of conductive

materials.[40-43] Especially, polyaniline (PANI) is one of widely investigated conductive polymers in various biomedical applications, due to its good biocompatibility and conductivity.[44-48] Our previous studies have demonstrated that blending PANI or incorporating oligoaniline into biomaterials performed the promoting effect on myotube formation or neurotrophin secretion,[48-52] and some other studies also confirmed that blending PANI into poly(lactic-co-glycolic acid) (PLGA) nanofibers could enhance the synchronized beating of CMs.[40] Thus, we hypothesis that blending PANI into polymer structures with nanofibrous architecture would be highly desirable to promote cardiac cell viability, maturation and function for cardiac tissue engineering, and furthermore to generate functionalized CMs-based bioactuators. On the other hand, due to the enhanced conductivity of polymer solution, the diameter of nanofibers decreased with the increase of PANI contents in electrospun solution under the same electrospinning process.[40] However, the fiber diameter of nanofibers has also been shown that can regulate and direct cell behavior. For instance, silk fibroin nanofibers with smaller diameter have been shown more favorable for the maturation of astrocytes. [53] Therefore, in order to study the influence of conductivity of nanofibers on cell behavior, the diameter should be controlled within same level to eliminate its effect. However, there are still few reports to individually investigate the effect of conductivity of nanofibrous structures on cardiac cell behavior. Furthermore, developing a CMs-based bioactuators by using conductive nanofibrous sheets has not been reported.

In this work, we reported a series of electrically conductive nanofibrous sheets with

the same fiber diameter for cardiac tissue engineering, and further utilized these conductive nanofibrous sheets to develop a series of CMs-based 3D bioactuators with spontaneous contraction motion, here exemplified by the conductive PLA/PANI nanofibrous sheets with different PANI contents prepared by electrospinning technique. Due to its good biocompatibility, degradability, controllable mechanical properties and thermoplastic properties, we used PLA to prepared PLA/PANI conductive nanofibrous sheets. To mimic the nanofibrous structure of myocardium ECM, the diameter of nanofibers was controlled within nanoscale (about 500 nm) and consistent by varying the voltage during electrospinning. H9c2 rat cardiomyoblasts were seeded on these PLA/PANI conductive nanofibrous sheets to investigate the cell viability, proliferation and differentiation. More importantly, primary CMs were cultured on these PLA/PANI conductive nanofibrous sheets to further investigate their cell viability, cytoskeleton organization, maturation and beating behavior. Furthermore, we also developed CMs-based 3D bioactuators with tubular and folding shape by utilizing these PLA/PANI conductive nanofibrous sheets as the fundamental materials, which were actuated by the spontaneous beating of CMs cultured on these sheets. We hypothesize that such PLA/PANI conductive nanofibrous sheets with ECM-liked nanostructure and conductivity that can provide a suitable microenvironment for cell viability, cytoskeleton organization, maturation and spontaneous beating of cardiac cells, will have a great potential for cardiac tissue engineering and CMs-bioactuators.

## 2 Materials and Methods

**2.1 Synthesis of PLA**

Polylactide with the molecular weight of 80,000 Da was prepared by ring opening polymerization (ROP) following our previous study.[54-56] In brief, the monomer L-LA and initiator ethylene glycol (EG) were added into a round-bottomed flask with a strict molar ratio in the presence of $Sn(Oct)_2$ as the catalyst. The reaction was carried out at 110 $^{o}$C under nitrogen atmosphere for 48 h. After reaction, chloroform was added to dissolve the resulting mixture, and the product was precipitated from chloroform in diethyl ether and finally vacuum dried for 48 h.

**2.2 Synthesis of PANI.**

PANI in the emeraldine salt (ES) form and emeraldine base (EB) form were synthesized according to our previous methods.[47, 48, 57] For the synthesis of PANI (ES), aniline (10 mmol) was dissolved in 0.1 mol/L HCl, and then ammonium persulfate (10 mmol) in 0.1 mol/L HCl solution was added into the reactor drop by drop during 30 min with magnetic stirring. After reacting for 4 h in air at room temperature, the resulting mixture was added into ethanol and then the PANI with ES form was collected after filtration. For the preparation of PANI (EB), PANI (ES) was treated with 0.1 mol/L $NH_4OH$ solution for 24 h at room temperature. The resulting PANI with EB form was filtered and washed by distilled water until the filtrate became neutral, and finally dried under vacuum for 72 h.

**2.3 Electrospinning of PLA/PANI nanofibrous sheet**

PLA/PANI nanofibrous sheets were prepared by employing an electrospinning process. In brief, equal amounts of PANI (EB) and camphorsulfonic acid (CSA) were

dissolved in a proper amount of hexafluoroisopropanol (HFIP) and then stirred for 12 h to obtain 0.7 wt% solution. The same procedure was employed to prepare about 10-19 wt% solutions of PLA in HFIP (Table 1). Then, the PANI solution was added into PLA solution with different volume ratios (Table 1), and the mixture solution was stirred for 12 h to obtain the PLA/PANI solution with different weight ratio. The final concentrations of PANI in PLA were set as 0 wt%, 1.5 wt%, and 3 wt%, respectively. Before electrospinning, the polymer solution was filtered through a 0.22 μm filter and then added to a 10 mL syringe with a 21 G hypodermic needle as the nozzle, and the volume flow rate of 1 mL/h was maintained using a syringe pump (Longer PrecisionPump, Baoding, China). For electrospinning, the voltages ranging from 12 kV to 16 kV were applied by using a high-voltage power supply (Dongwen High Voltage Power Supply Plant, Tianjin, China). A metal platform was used as the collector that wrapped with aluminium foil and located at a fixed working distance of 15 cm from the needle tip. In order to prepare the PLA/PANI nanofibrous sheets on the cover glass slips (diameter 22 mm), the glass slides were placed on the surface of the metal platform to collect nanofiber random web during the electrospinning (Fig. 1a). The samples with the PANI contents of 0 wt%, 1.5 wt%, and 3 wt%, were named as PLA, PLA/PANI1.5, and PLA/PANI3, respectively. All the nanofibrous sheets were dried under vacuum at room temperature for 24 h to remove any solvent residue before use.

**2.4 Characterization of nanofibrous sheets**

The micro-morphology of electrospun nanofibrous sheets was analyzed by scanning

electron microscope (SEM) (Quanta FEG 250, FEI) at an accelerating voltage of 5 kV.

Water contact angle of nanofibrous sheets was recorded by using sensible drop method ($n > 6$ per sample). A droplet of deionized water was deposited on the sample using 21 G needle and high-resolution image of the droplet was captured and analyzed after 10s.

Cyclic voltammetry (CV) of PLA/PANI was conducted on an Electrochemical Workstation employing a three-electrode system. PLA/PANI polymer solution was dropped on an indium tin oxide (ITO) glass followed by solvent evaporation to obtain films. The ITO glass coating with PLA/PANI film was immersed in dimethyl sulfoxide (DMSO)/0.5 mol/L CSA solution and served as working electrode, and an Ag/AgCl served as reference electrode, and a platinum disk served as counter electrode, respectively. The CV of PLA/PANI was measured on an Electrochemical Workstation (CH Instruments) with a scan rate of 50 mV/s.

The electrical conductivity of PLA/PANI samples with diameter of 22 mm and 2 μm thickness doped with CSA were measured by the standard Van Der Pauw DC four-probe method. For the measurement, a corresponding electrical current was obtained when provide a voltage for the square sample. The electrical conductivity of these samples was calculated by the following formula: $\sigma\ (S/cm) = (2.44 \times 10/S) \times (I/E)$, where $\sigma$ is the conductivity, S is the side area of square sample, I is the current passed through outer probes, and E is the voltage drop across inner probe.

**2.5 Cell isolation and culture**

H9C2 rat cardiomyoblasts were purchased from Shanghai cell bank of Chinese Academy of Sciences. H9c2 cells were cultured with Dulbecco's Modified Eagle Medium (DMEM, GIBCO) supplemented with 10 % fetal bovine serum (FBS, BI), 100 U/mL penicillin and 100 U/mL streptomycin in an incubator at 37 $^{o}$C in 5 % $CO_2$. After the confluence reached 90 %, cells were passaged at a passage ratio of 1:3.

Neonatal primary CMs were isolated from the hearts of 2-day-old Sprague-Dawley rats according to an established method.[27] Briefly, hearts were cut into pieces and suspended in 0.1 % collagenase type 2 (GIBCO) dissolved in Dulbecco's phosphate-buffered saline (DPBS). Digestion was carried out in a water bath at 37 $^{o}$C for serval times. After digestion, the supernatant was collected and centrifuged at 1200 rpm for 5 min. Cells were resuspended in culture medium and plated in Petri dish. To selective enrich CMs, cells were preplaced for 1 h to eliminate the contamination of cardiac fibroblasts.

**2.6 H9c2 cell viability and proliferation on nanofibrous sheet**

H9c2 cells viability tests were performed by using a live/dead viability kit (Molecular Probes). The nanofibrous sheets were sterilized by 75 % ethanol and soaking in culture medium for 2 h before seeding cells. H9c2 cells were seeded on sterilized nanofibrous sheets at a density of 6000 cells/cm$^2$ and cultured in 12 wells plate ($n > 3$). After culture for 24 h, the cells were washed by DPBS for three times and then treated with ethidium homodimer-1 (0.5 μM) and calcein AM (0.25 μM) for 45 min at 37 $^{o}$C. The cells were observed under an inverted fluorescence microscope (IX53, Olympus). Living cells which were stained with calcein AM, showed green color, while dead

cells which were stained with ethidium homodimer-1 showed red color under the fluorescence microscope. The quantitative analysis of the cell viability on PLA/PANI1.5 and PLA/PANI3 nanofibrous sheets were comparable to the PLA nanofibrous sheets.

The proliferation rate of H9c2 cells on nanofibrous sheets was evaluated by Alamar Blue assay (Molecular Probes). Briefly, H9c2 cells were seeded on nanofibrous sheets at a density of 6000 cells/cm$^2$, and medium was changed every day ($n > 3$). At each time point of assay, the culture medium was replaced with medium containing 10% (v/v) Alamar Blue reagent at 37 $^{o}$C in 5% $CO_2$ for 4 h, then 100 uL solution from each example was removed into a 96 wells plate and read at 530/600 nm in a SpectraMax fluorescence microplate reader (Molecular Devices). Medium containing 10% (v/v) Alamar Blue reagent served as blank.

**2.7 CMs cell viability and cytoskeleton organization on nanofibrous sheet**

CMs viability tests were also performed by using a live/dead viability kit (Molecular Probes) following the same procedure with H9C2 which described above. Briefly, CMs were seeded on sterilized nanofibrous sheets at a density of 10000 cells/cm$^2$ and cultured in 12 wells plate ($n > 3$). After culture for 36 h, the cells were washed by DPBS for three times and then treated with ethidium homodimer-1 (0.5 μM) and calcein AM (0.25 μM) for 45 min at 37 $^{o}$C. CMs were observed under an inverted fluorescence microscope (IX53, Olympus). To visualized the cytoskeleton organization of CMs on nanofibrous sheets, CMs were fixed at day 2 with 4% paraformaldehyde for 15 min. CMs were then treated with 0.1% Triton X-100 for 45

min. After permeabilizing, fluorescein Isothiocyanate (FITC) labeled phalloidin (sigma) were pipetted into the samples for 90 min. Cell nuclei were counterstained with DAPI before observation using a confocal laser microscope (FV1200, Olympus). FFT analysis was performed by using ImageJ software based on F-actin fluorescence images to assess the organization of F-actin in each sample. Aspect ratio of cells was determined by calculating the ratio between the length of the longest line and the length of the shortest line across the nuclei. The data were collected from at least three images for three replicated samples of each group.

**2.8 Immunofluorescence staining**

For immunofluorescence staining, the cells on nanofibrous sheets were rinsed twice gently with DPBS and then fixed with 4% paraformaldehyde for 15 min at room temperature. The fixed cells were then rinsed twice gently with DPBS and treated with 0.1% Triton X-100 for 45 min. After being blocked in 5% goat serum in DPBS for 1 h, H9c2 cells were incubated in rabbit anti-MYH2 (myosin heavy chain 2) antibody (Santa Cruz), while CMs were incubated with mouse anti-α-actinin antibody (abcam) and rabbit anti-connexin43 antibody (abcam) at 4 $^{o}$C overnight. After being washed with DPBS, Alexa Fluor 488 conjugated secondary antibody (Molecular Probes) and Alexa Fluor 594 conjugated secondary antibody were added and incubated for 1.5 h at room temperature. Cell nuclei were counterstained with DAPI before observation using a confocal laser microscope (FV1200, Olympus). For quantification of α-actinin and connexin43 area coverage, the fluorescent images of α-actinin and connexin43 staining were taken at 20 X magnification. Then the area

fraction covered by α-actinin and connexin43 were quantified by using ImageJ software, respectively. The myotube data were analyzed by using ImageJ software, and the data came from three images for three replicated samples in each group.

**2.9 Beating behavior of CMs on nanofibrous sheets**

The inverted microscope was equipped with a charge-coupled device (CCD) camera to record the beating video of CMs on nanofibrous sheets 21 days of cultivation. Three samples for each group were recorded and their beating frequencies were presented as beating time per minute. The video sequences were digitized at a rate of 24 frames per second. The beating signal patterns of CMs on nanofibrous sheets at day 6 and day 21 were obtained using a custom written MATLAB program.[58]

**2.10 Calcium transients imaging**

After 8 days of culturing, the nanofibrous sheets were stained with 5 μm Fluo-4 AM (Molecular probes) to visualize the calcium transients according to the manufacturer's instructions. Briefly, after removed culture medium, the sheets were washed two times with Tyrode's solution and treated with 5 μM Fluo-4 AM (prepared in Tyrode solution) for 30 min at 37 $^{o}$C in 5% $CO_2$. After staining, the sheets were washed with Tyrode's solution and calcium transients were recorded under a fluorescence microscope with a × 40 objective lens (Olympus, BX53). Three replicated samples were examined for each group, and at least three regions were recorded for each sample. Data analysis was performed using ImageJ software. For image analysis, three independent regions of interest (ROI) were randomly selected and analyzed. The background fluorescence was subtracted from the mean fluorescence in the ROI, giving a background-corrected

normalized fluorescence value. Changes of the [$Ca^{2+}$] are expressed as $F/F_0$, where F is the fluorescence intensity at intermediate calcium levels, and $F_0$ is the baseline fluorescence intensity.

**2.11 Preparation and characterization of bioactuators**

The tubular and folding shaped bioactuators were prepared by the CMs-laden nanofibrous sheets. After cultured CMs on PLA and PLA/PANI3 nanofibrous sheets for 6 days, the CMs laden-sheets were detached from the glass slide and then prepared to tubular and folding shaped 3D bioactuators. Briefly, due to the tensile force in liquid, the CMs laden-sheets with round shape stretched well in culture medium, then two fine forceps were used to fold the sheet along the diameter into a semicircle and fold it again into a quarter circle. After that, a folding shaped 3D bioactuator was formed. Tubular shaped 3D bioactuators were also prepared by using two fine forceps. After detaching a CMs laden-sheet from the glass slide, two fine forceps clamped the edge of the sheet, then griped these forceps and rolled them carefully at the same time, the sheet would consequently have been rolled into a tube and transformed into a tubular shaped 3D bioactuator. 3D bioactuators were continuously cultured in culture medium for 4 days to allow the CMs adopt the new microenvironment of tubular and folding shapes and spontaneously beating. The inverted microscope was equipped with a CCD camera to record the contraction video of these 3D bioactuators. The actuation of those bioactuators were estimated by measuring the contraction frequency and the displacement of tubular and folding bioactuators directly from sequential video frames every 0.042 second. The contraction frequency and signal

patterns were analyzed by a MATLAB program as described in a previous study.[58]

### 2.12 Statistical analysis

Experiments were run in triplicate for each sample, and results are presented as mean ± standard deviation. Statistical differences were obtained through analysis of variance followed by students't-test. A significance level of 0.05 was applied to determine significant differences.

## 3 Results and Discussion

### 3.1 Preparation and characterization of PLA/PANI nanofibrous sheet

In this work, we aim to fabricate a series of electroactive nanofibrous scaffolds to engineer the cardiac tissue and CMs-based 3D bioactuators. PLA and PANI were chosen as raw materials because PLA shows good biocompatibility and degradability, and PANI exhibits good conductivity and biocompatibility. PLA/PANI nanofibrous sheets with different PANI contents were prepared by an electrospinning process as illustrated in Figure 1a. To investigate the cell behavior on the surface of nanofibrous sheets more conveniently, these PLA/PANI nanofibrous sheet samples were collected on glass slips with 22 mm diameter. As shown in Figure 1b, the optical images showed that these nanofibrous sheets were placed on glass slips very well, and the higher PANI content in nanofibers exhibited the darker green color compared to the PLA nanofibrous sheet with white color. These nanofibrous PLA, PLA/PANI1.5 and PLA/PANI3 samples showed the similar thickness approximate 2 μm by controlling the same electrospinning time. For electrospinning, the composition of electrospun solution and electrospinning situations including voltage, volume flow rate, collection

distance, and temperature would contribute to the diameter of nanofibers.[31-34] Previous studies have demonstrated that the addition of conductive materials such carbon nanotubes (CNT) and PANI within electrospun solution could decrease the nanofibrous diameter under the same electrospinning process due to the enhanced conductivity of polymer solution.[40, 42, 59] On the other hand, the diameter of nanofibers has also been regarded as an important parameter for regulating cell maturation and behavior.[53] Therefore, in our study, in order to investigate the effect of conductivity rather than the diameter size of these conductive nanofibrous sheets on CMs function and differentiation, all the diameters of these nanofibrous sheets were controlled within the same range about 500 nm via regulating the electrospun voltage ranging from 12 to 16 kV (Fig. 1c-f). The SEM images of these nanofibrous sheets exhibited the uniform random nanofibrous microstructure with similar diameters and the statistical results also showed that there was no significant difference of nanofiber diameters between groups (Fig. 1c-e). The surface hydrophobicity-hydrophilicity of electrospun nanofibrous scaffolds also plays a critical role in cell adhesion and proliferation behavior because the hydrophilicity would have an effect on the surface energy and therefore might influence the serum proteins to adhere on scaffolds.[60] The water contact angles of PLA/PANI1.5 and PLA/PANI3 were $120 \pm 8^{o}$ and $113 \pm 5^{o}$, respectively, which were slightly lower than that of PLA sheet ($128 \pm 6^{o}$) (Fig. 1g). Furthermore, all of these nanofibrous sheets showed the lower water contact angles after immersing in medium for 24 h. Especially, the water contact angles of PLA/PANI1.5 and PLA/PANI3 significantly

decreased to 100 ± 7° and 94 ± 6°, respectively. In our previous study, we found that incorporation of electrical conductive segments such as aniline tetramer (AT) significantly increased protein adsorption because the electrostatic force increased as AT segments increased in the copolymers. [62] Therefore, the increase of hydrophilicity suggested that the presence of PANI within nanofibers might have a positive effect on protein adhesion within medium.[61] The electrochemical properties of PLA/PANI samples were investigated by cyclic voltammetry (CV) (Fig. 1h, Fig. S1). For instance, for the CV curves of PLA/PANI3 films doped with CSA (Fig. 1h), there are two pairs of oxidation/reduction peaks at 0.21 V and 0.53 V, which were assigned to the transition from the leucoemeraldine oxidation state to the emeraldine oxidation state, and then from the emeraldine oxidation state to the pernigraniline state, respectively. These CV results showed the typical electrochemical properties of PANI, which agreed well with previous reports about the CV analysis of PANI-based materials.[46] In addition, the CV spectra measured by multiple cycles further suggested their stable electrochemical properties. Moreover, the conductivities of the PLA/PANI1.5 and PLA/PANI3 doped with CSA were 3.6 ± 0.7 × $10^{-6}$ S/m and 2.1 ± 0.3 × $10^{-5}$ S/m (Fig. 1i). The conductivity of these nanofibrous sheets increased with the increase of PANI content, because the higher PANI content would more easily form a conductive network within blending system to promote the electrical conductivity. These samples showed the relatively low conductivities value, but are sufficient for the conduction of electrical signal in vivo or cell communication, based on our previous work and some other studies about the

conductive biomaterials for tissue engineering applications.[52, 62]

### 3.2 Cell viability, proliferation and differentiation of H9c2 cells on nanofibrous sheets

To evaluate whether these PLA/PANI nanofibrous sheets could be used in cardiac tissue regeneration, we first cultured a rat cardiomyoblast cell line (H9c2) on these conductive nanofibrous sheets. H9c2 cells were chosen because H9c2 cells were widely used in many studies to evaluate the effect of biomaterials on cardiac cells proliferation, and it is commercially available.[63] After seeding for 24 h, the Live/Dead staining was performed to visualize the cell viability of H9c2 cells on these conductive nanofibrous sheets. The majority of cells on PLA/PANI1.5 and PLA/PANI3 nanofibrous sheets showed green fluorescence which indicated alive. The quantitative analysis of cell viability on PLA/PANI1.5 and PLA/PANI3 nanofibrous sheets was comparable to the PLA nanofibrous sheets (Fig. S2b), which is a FDA approved biomaterials. Although the water contact angles of PLA/PANI sheets decreased with the increase of PANI contents, the difference in cell number between PLA and PLA/PANI were not observed, because hydrophobicity, composition and surface charge of the nanofibers all affected the cell adhesion. H9c2 cells proliferation during 3 days of culturing was further examined in this study. There was no significant difference in cell proliferation rate among nanofibers at each time point (Fig. S2c). These results demonstrated that PLA/PANI nanofibrous sheets showed the good cell viability and proliferation similar to PLA nanofibrous sheets.

We further investigated the myogenic differentiation of H9c2 cells on these

conductive nanofibrous sheets. After induction, multinucleated fused myotubes with highly organized structure were formed on PLA/PANI1.5 and PLA/PANI3 nanofibrous sheets, which were visualized by immunofluorescence staining of MYH2 (Fig. 2a, Fig. S3). To quantitatively analyze the effect of PLA/PANI nanofibrous sheets on the differentiation of H9c2 cells, the length, diameter, number, maturation index and fusion index of myotubes were measured. After 6 days in the differentiation medium, there was no significant difference of the myotube diameter in these PLA/PANI nanofibrous sheet groups (Fig. 2d). Comparatively, the myotube length on the PLA/PANI1.5 (1313.1±146.5 μm) and PLA/PANI3 (911.3±179.7 μm) were significantly much longer than that on the PLA (632.1±117.4 μm) (Fig. 2b) and that reported in other nanofiber study.[64] In addition, the H9c2 cells on the PLA/PANI1.5 and PLA/PANI3 nanofibrous sheets formed more myotubes than that on PLA nanofibrous sheets (Fig. 2c). Particularly, the maturation index as another differentiation parameter to evaluate the maturation of myotubes by measuring the percentage of myotubes with more than 5 nuclei was analyzed. The results showed that more mature myotubes were formed on PLA/PANI1.5 and PLA/PANI3 (above 75 % and 73 %, respectively), while only 34 % of myotubes formed on PLA nanofibrous sheets were mature (Fig. 2e). Moreover, the fusion index of cells on these samples was also measured as a key index to evaluate the fusion of myotubes. As shown in Figure 2f, the fusion index of PLA group was 50%, which showed the similar fusion index to other nanofibrous scaffolds in some previous reports. [65] Contrastively, the fusion index of PLA/PANI1.5 and PLA/PANI3 significantly

increased into 75.2% and 73.7%, respectively. In previous studies, the nanofibrous structure has been demonstrated that could promote fusion index of H9c2 cells compared with flat polymer films.[65] On the other hand, incorporating of the conductivity properties into biomaterials also has been regarded as an effective approach to enhance myotubes formation.[66] In our study, PLA/PANI groups showed the higher fusion index compared with PLA group and some other nanofibrous scaffolds in previous studies, which mainly contributed to the synergetic effect of nanofibrous structure and conductive properties. These data demonstrated that these PLA/PANI conductive nanofibrous sheets have promoting effect on differentiation of H9c2 cells in terms of myotube number, myotube length, maturation index and fusion index. These results further suggested the great potential of these PLA/PANI nanofibrous sheets for cardiac tissue engineering applications.

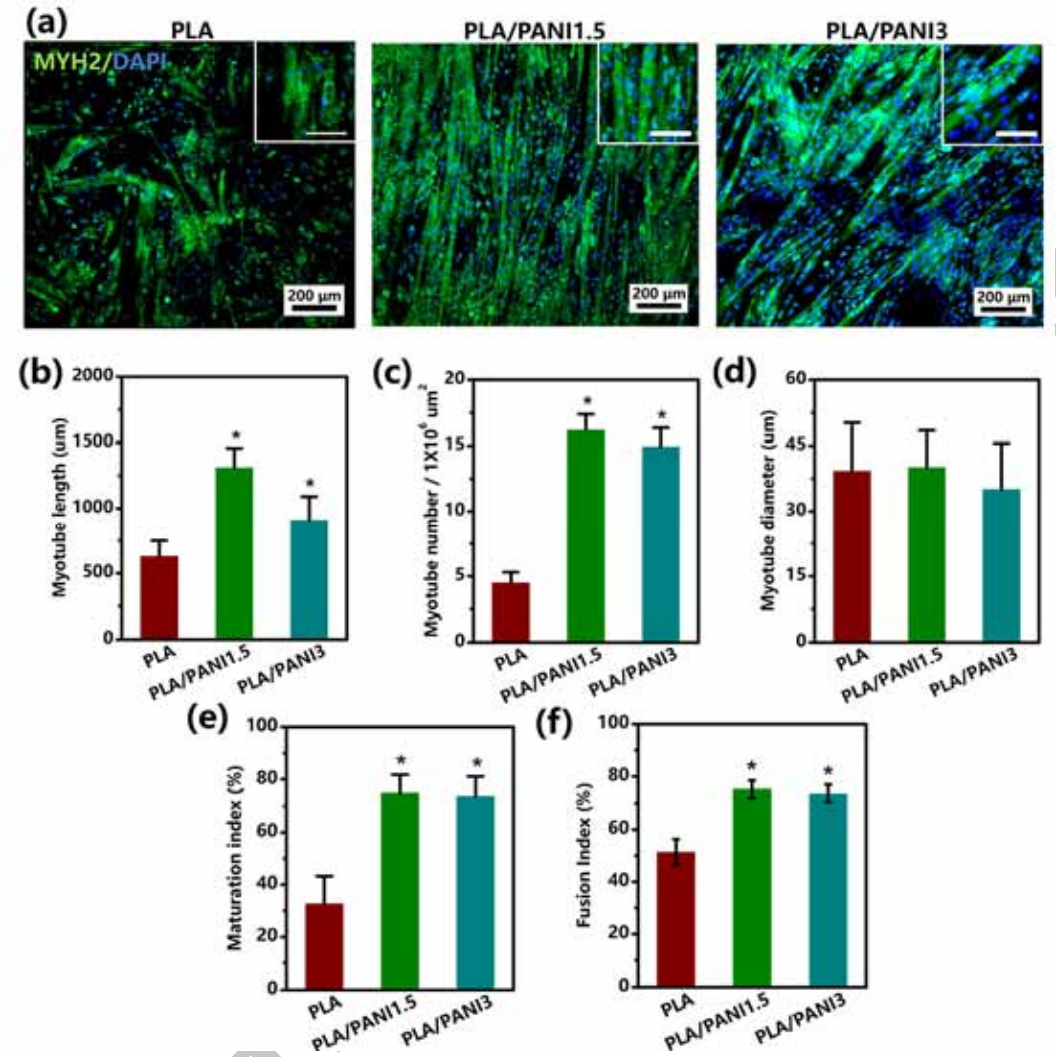


**Figure 2.** The immunofluorescence staining of MYH2 (green) showed the myotube formation of H9c2 cells on PLA/PANI nanofibrous sheets after 6 days of differentiation (a). The quantitative results of myotube length (b), myotube number (c), myotube diameter (d), maturation index (e) and fusion index (f) were analyzed after 6 days of differentiation. *$P$<0.05.

### 3.3 Cell viability and actin cytoskeleton organization of CMs on PLA/PANI nanofibrous sheets

After confirmed the good compatibility of PLA/PANI nanofibrous sheets in terms of proliferation and enhanced differentiation of H9c2 cardiomyoblasts, we further

investigate the cell behavior of primary CMs on these nanofibrous sheets, because CMs are the major muscle cells that make up the cardiac muscle in heart and utilized in many studies for cardiac regeneration.[6, 7, 24, 40] Similarly, live/dead staining results showed that the majority of CMs on PLA/PANI nanofibrous sheets were alive and vibrant after 36 h (Fig. S4a). The quantitative analysis also confirmed the good cell viability of CMs on PLA/PANI1.5 and PLA/PANI3 nanofibrous sheets, compared with that on PLA nanofibrous sheets (Fig. S4b). To evaluate the effect of PLA/PANI nanofibrous sheets on cell morphology, confocal fluorescence images of F-actin (green) and DAPI (blue) staining were taken to visualize the cytoskeleton organization of CMs on the samples after culturing for 48 h. CMs on PLA nanofibrous sheets had limited expression of F-actin fibers and exhibited a rectangle morphology (Fig. 3a). Contrastively, CMs on PLA/PANI1.5 and PLA/PANI3 nanofibrous sheets expressed much more F-actin fibers across all the geometrical features (Fig. 3a). Moreover, elongated CMs with well-defined stress fibers were both observed on PLA/PANI1.5 and PLA/PANI3 nanofibrous sheets, while they were elusive on PLA nanofibrous sheets (Fig. 3a). Additionally, fast Fourier transform (FFT) analysis of F-actin fiber showed that the CMs on PLA/PANI3 were clearly interconnected and locally aligned (Fig. 3a, top right insets), which indicated the better cell-cell interactions. To further evaluate the quantification of local cell alignment, cellular orientation distribution and aspect ratio derived from F-actin staining images were investigated (Fig. 3b, d). The analysis results showed that the cellular orientation distribution and aspect ratio were both enhanced by the increase of

PANI contents in these nanofibrous sheets, which might be due to the positive effect of the conductivity of nanofibers on the good cellular organization. These data showed that these nanofibrous sheets composed of PANI and PLA polymer provided a conductive and biocompatible nanofibrous microenvironment for CMs cultivation and further performed the ability to enhance cellular spreading and alignment and cell-cell interactions when CMs were cultured on PLA/PANI nanofibrous sheets.

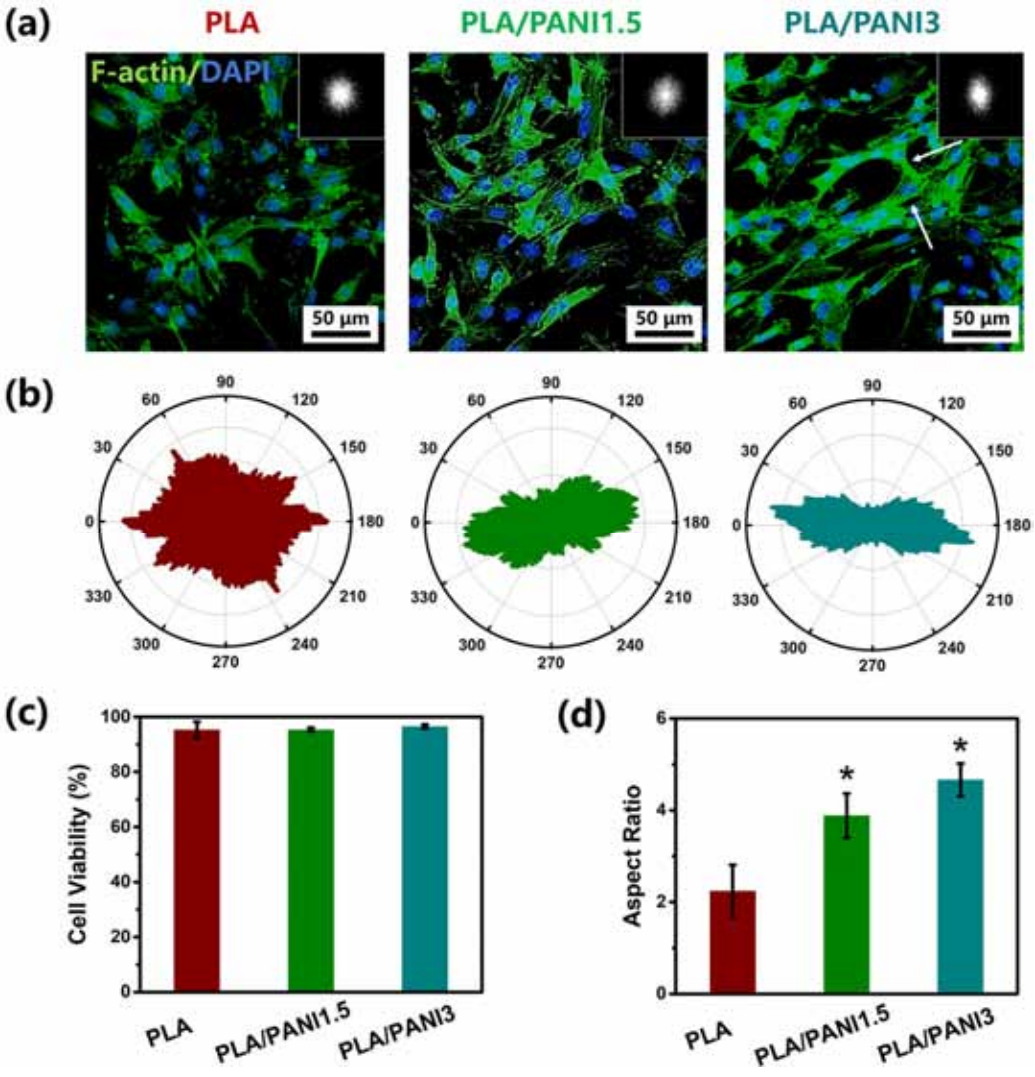


**Figure 3.** The cell viability and morphology of cardiomyocytes on PLA/PANI nanofibrous sheets after culture for 2 days. Cardiomyocytes showed good cell

viability on PLA/PANI nanofibrous sheets (c). The morphology of cardiomyocytes was visualized by the immunofluorescence staining of F-actin (green) (a). Insets are corresponding FFT images. White arrows showed the interconnected cells. Cellular orientation distribution derived from F-actin staining images were present (b). Aspect ratio was also analyzed (d). *$P$<0.05.

**3.4 Maturation, beating behavior and calcium transients of CMs on PLA/PANI nanofibrous sheets**

The functional and biological behavior of CMs on PLA/PANI nanofibrous sheets were further investigated in terms of maturation and beating behavior. The maturation of CMs on PLA/PANI nanofibrous sheets was visualized by immunofluorescence staining for cardiac-specific proteins, sarcomeric α-actinin and connexin 43 (CX43). The sarcomeric α-actinin is a key marker for the maturation and strong contractility of CMs,[67] and CX43 is a gap junction protein which is responsible for cell-cell coupling and synchronous beating of CMs.[68] After 8 days of culturing, the CMs on PLA/PANI1.5 and PLA/PANI3 nanofibrous sheets exhibited pervasive interconnected sarcomeric structures with partial uniaxial alignment (Fig. 4b, c). However, cells on PLA nanofibrous sheets just showed scattered and poorly organized sarcomeric structure (Fig. 4a). This finding indicated that CMs on PLA/PANI nanofibrous sheets expressed more homogeneously organized sarcomeric α-actinin than that on PLA nanofibrous sheets, which was in accordance with the cytoskeleton organization of CMs revealed by F-actin (Fig. 3a). Furthermore, the quantitative analysis results showed that the area coverage of sarcomeric α-actinin on PLA/PANI1.5 and

PLA/PANI3 nanofibrous sheets were significantly higher (46.74% and 51.04%, respectively) than that on PLA nanofibrous sheets (32.52%) (Fig. 4d). Similarly, CX43 was well expressed and showed much more homogeneous distribution on PLA/PANI1.5 and PLA/PANI3 nanofibrous sheets. From the higher magnification images, it was shown that the CX43 were mainly distributed between adjacent CMs on PLA/PANI1.5 (Fig. S5b) and PLA/PANI3 (Fig. S5c). In contrast, only sparse distribution of CX43 was observed in CMs on PLA nanofibrous sheets (Fig. 4a and Fig. S5a). The area coverage of CX43 on PLA/PANI1.5 and PLA/PANI3 nanofibrous sheets were notably higher (4.1 times and 3.9 times, respectively) than that on PLA nanofibrous sheets ($P$<0.05). Increase of CX43 expression indicated better cell-cell interaction in PLA/PANI nanofibrous sheets. These immunofluorescence staining results indicated the well-developed networks of sarcomeres and gap junctions and the suitability to induce synchronized beating of CMs on PLA/PANI nanofibrous sheets, which provide the conductivity and ECM-liked nanostructure.

The spontaneous beating behavior of CMs was further investigated to evaluate the CMs biological behavior on PLA/PANI nanofibrous sheets for 21 days of culturing. CMs grown on PLA/PANI1.5 and PLA/PANI3 nanofibrous sheets displayed more synchronous beating with much higher beating rate than that on PLA nanofibrous sheets as early as 4 days (Fig. 5a). During the period of culturing, it was found that CMs on both PLA/PANI1.5 and PLA/PANI3 sheets showed the spontaneous beating as high as 81 beats $min^{-1}$ and 115 beats $min^{-1}$ at day 4, respectively. Contrastively, their spontaneous beating decreased to 23 beats $min^{-1}$ and 28 beats $min^{-1}$ at day 14,

because CMs needed a period of time to adopt the microenvironment of PLA/PANI sheets and establish cell-cell interactions with adjacent cells. However, the number of beats of CMs on PLA/PANI1.5 and PLA/PANI3 sheets increased to 58 beats $min^{-1}$ and 68 beats $min^{-1}$ after 14 days' cultivation, which was mainly contributed by the good cell-cell coupling during this time. In contrast, due to the less spreading of cells, poor cytoskeletal organization (Fig. 3a) and the lack of cell-cell interactions (Fig. 4a), CMs on PLA nanofibrous sheets exhibited irregular spontaneous beating with lower beating frequency (13-38 beats $min^{-1}$) during 21 days of culturing (Fig. 5a). Moreover, CMs on PLA nanofibrous sheets had irregular contraction patterns and did not beat synchronously during the whole culturing period (Movie S1, S4). However, CMs grown on PLA/PANI1.5 and PLA/PANI3 nanofibrous sheets displayed more synchronous beating after culture for 6 days and even 21 days (Fig. 5b, c, and Movie S2, S3, S5, S6). These results suggested that these PLA/PANI nanofibrous sheets based on PANI component and PLA polymer can maintain the synchronous beating of CMs for at least 3 weeks.

The calcium transients of CMs on PLA/PANI nanofibrous sheets were also examined using calcium-sensitive dye Fluo-4 AM. After stained with Fluo-4 AM, the spontaneous calcium oscillations on PLA, PLA/PANI1.5 and PLA/PANI3 sheets were recorded (Fig. 6 and Movie S7). Three independent ROI were randomly selected and analyzed (Fig. 6a-c). Spontaneous calcium transients were captured by line scanning across multiple cells in ROI, and showed the calcium sparks during beating (Fig. 6d-f). Spontaneous calcium transients in neighboring cells of PLA/PANI1.5 and

PLA/PANI3 groups were synchronized with three independent ROI, while asynchronous calcium transients occurred in PLA group (Fig. 6d-f). Consistently, dynamic changes of $Ca^{2+}$ corresponding to calcium sparks (Fig. 6g-i) also revealed the more synchronized calcium transients in PLA/PANI1.5 and PLA/PANI3 groups, compared with that in PLA group. These results demonstrated that the PLA/PANI nanofibrous sheets with conductivity promoted the formation of electrical coupling of CMs during spontaneous beating.

Together, these PLA/PANI conductive nanofibrous sheets not only provided a ECM-liked nanoscale microenvironment for cell adhesion and maturation, but also rendered superior electrical cell-cell coupling for synchronous beating and calcium transients enabled by good cell-cell interactions compared with PLA nanofibrous sheets. Furthermore, the CMs on PLA/PANI conductive nanofibrous sheets could continue beating spontaneously with regular contraction patterns even after culturing for 21 days (Fig. 5c, and Movie S5, S6), and therefore such spontaneously regular contraction behavior for a long term exhibited the promising potential of these nanofibrous sheet for engineering functional cardiac constructs in clinical applications.

**3.7 CMs-laden PLA/PANI nanofibrous sheets as bioactuators**

Integration of CMs and polymer-based scaffolds has been recently regarded as a promising approach for creating various bioactuators that can be actuated without any other external stimulations, because the spontaneously regular contraction behavior of CMs can convert chemical energy of glucose into mechanical energy.[22] Many

reports have focused on utilizing PDMS as fundamental material to create CMs-based bioactuators.[15, 23] Although PDMS could be easily fabricated with different modulus or structures, its hydrophobicity and the lack of nanofibrous structures that mimic ECM to favor CMs contraction limited its wide application. In addition, to improve the functionality of CMs-based bioactuators, conductive materials such as CNT or graphene were incorporated into the scaffolds to increase their conductivity.[69] Thus, developing a CMs-based bioactuators that exhibited the nanofibrous structure and conductivity would be highly beneficial, while still remains a great challenge.

In this study, we suppose that PLA/PANI conductive nanofibrous sheets which possessed ECM-liked nanofibrous structure and conductivity, should be a suitable fundamental material to generate CMs-based 3D bioactuators, because CMs cultured on PLA/PANI conductive nanofibrous sheets showed good cell viability, good cellular organization, well-developed networks of sarcomeres and gap junctions, and exhibited spontaneously beating during 21 days of culturing. To confirm this hypothesis, we used PLA/PANI3 conductive nanofibrous sheets to fabricate 3D bioactuators with tubular shape and folding shape, and the PLA nanofibrous sheets served as control group. After cultured CMs on PLA/PANI nanofibrous sheets for 6 days, the CMs-laden sheets were detached from the glass slide and then tubular and folding shaped 3D bioactuators were prepared by using fine forceps (Fig.7a). These 3D bioactuators were continuously cultured in culture medium for 4 days to allow the CMs adopt the new microenvironments and then spontaneously beating. As shown in

the contraction video, the actuation of those bioactuators was estimated by measuring the contraction frequency and the displacement of tubular and folding bioactuators directly from sequential video frames every 0.042 second. After 4 days of culturing, the tubular shaped 3D bioactuators formed by PLA/PANI3 conductive nanofibrous sheets (Fig. 7b (iv), (v)) displayed strong spontaneous contraction at 1.6 Hz and displacement without any trigger (Movie S8), which was driven by synchronous beating of the CMs. In contrast, weak spontaneous contraction at 0.6 Hz was observed in tubular shaped 3D bioactuators formed by PLA nanofibrous sheets (Fig. 7b (i), (ii)) (Movie S9). In details, the maximum displacement was much higher in tubular shaped 3D bioactuators formed by PLA/PANI3 conductive nanofibrous sheets (6.9 μm) (Fig. 7b (vi)) than that in tubular shaped 3D bioactuators formed by PLA nanofibrous sheets (4.0 μm) (Fig. 7b (iii)). Therefore, tubular shaped bioactuators formed by PLA/PANI3 conductive nanofibrous sheets, which rendered superior electrical cell-cell coupling for synchronous beating of CMs, showed stronger contraction and higher displacement compared with the bioactuators formed by PLA nanofibrous sheets. Folding shaped 3D bioactuators formed by PLA/PANI3 conductive nanofibrous sheets (Fig. 7c (iv), (v)) also displayed strong spontaneous contraction at 1.2 Hz and the maximum displacement was 5.9 μm (Fig. 7c (vi)) (Movie S10). However, no obvious contraction could be observed in folding shaped bioactuators prepared by PLA nanofibrous sheets (Fig. 7c (i), (ii)) (Movie S11), and the displacement was slight and irregular (Fig. 7c (iii)).

The contraction frequency and displacement differed depending on the conductivity

of nanofibrous sheets and the shape of bioactuators. CMs cultured on PLA/PANI3 conductive nanofibrous sheets which could continue beating spontaneously with regular contraction patterns at high frequency, directly contributed to the strong spontaneous contraction at relative high frequency of both tubular and folding shaped bioactuators formed by PLA/PANI conductive nanofibrous sheets. Meanwhile, for PLA/PANI3 and PLA nanofibrous sheets, the shape of bioactuators could also influence the contraction frequency and displacement. For example, tubular shaped bioactuators formed by PLA/PANI3 displayed more strong beating at higher frequency (1.6 Hz) with higher maximum displacement (6.9 μm) than folding shaped bioactuators (1.2 Hz, 5.9 μm). The hollow structure of tubular shaped bioactuators, which provided enough space for nutrition exchange and oxygen entrance, may contribute to the superior promoting effect on the beating frequency and displacement. These results suggest that PLA/PANI conductive nanofibrous sheets have great potential as CMs-based 3D bioactuators.

The CX43 immunostaining results may explain the reason of how the conductivity of nanofibrous sheets influence the beating frequency and displacement of 3D bioactuators (Fig. 8). Strong positive staining for CX43, a gap junction protein which is responsible for cell-cell coupling and synchronous beating of CMs, were exhibited on tubular and folding shaped bioactuators formed by PLA/PANI3 conductive nanofibrous sheets (Fig. 8b, d). Besides, the homogeneous distribution of CX43 on folding shaped bioactuators may result from the flat structure of folding shape, while the heterogeneous distribution of CX43 on tubular shaped bioactuators resulted from

the hollow and curved structure of tubular shape. In comparison, both tubular shaped and folding shaped bioactuators formed by PLA nanofibrous sheets showed much weaker staining for CX43 (Fig. 8a, c). These results indicated good cell-cell coupling for electric propagation for PLA/PANI3 group than that of PLA group, which agreed with the CX43 staining results of CMs cultured on nanofibrous sheets fixed on glass slide (Fig. 4), and further demonstrating the great potential of PLA/PANI conductive nanofibrous sheets as CMs-based 3D bioactuators.

**Conclusion**

We demonstrated that the polylactide/polyaniline (PLA/PANI) electrically conductive nanofibrous sheets with similar nanofiber diameter provide a conductive and biocompatible nanofibrous microenvironment for CMs viability, maturation and synchronized beating, also displayed the great potential of PLA/PANI conductive nanofibrous sheets as CMs-based 3D bioactuators. The electrospun PLA/PANI conductive nanofibrous sheets with different PANI contents were tuned with the same fiber diameter. These PLA/PANI nanofibrous sheet with conductivity and ECM-liked nanostructure showed good biocompatibility and promoting effect on differentiation of H9c2 cells in terms of myotube number and maturation index. Moreover, primary CMs exhibited increased cellular spreading and alignment and cell-cell interactions with the increase of PANI contents, when cultured on PLA/PANI conductive nanofibrous sheets. Immunofluorescence staining results also demonstrated well-developed networks of sarcomeres and gap junctions of CMs on PLA/PANI conductive nanofibrous sheets, compared with that on PLA nanofibrous sheets. The

CMs on PLA/PANI conductive nanofibrous sheets could continue beating spontaneously with regular contraction patterns after 21 days of culturing. These results suggest that PLA/PANI conductive nanofibrous sheets exhibited the promising potential in cardiac tissue engineering. Furthermore, when released from glass slide, CMs-laden PLA/PANI3 conductive nanofibrous sheets can form 3D bioactuators with tubular and folding shapes, and spontaneous contraction with much higher frequency and displacement than that on CMs-laden PLA nanofibrous sheets. Therefore, PLA/PANI conductive nanofibrous sheets further displayed the great potential as CMs-based 3D bioactuators.

**Acknowledgements**

The National Natural Science Foundation of China (grant number: 51673155) and Xi'an Jiaotong University were acknowledged for financial support of this work.

**Supporting Information**

Supporting Information is available.

**References**

[1] Mendis S. Global status report on noncommunicable diseases 20142014.

[2] Bui AL, Horwich TB, Fonarow GC. Epidemiology and risk profile of heart failure. Nat. Rev. Cardiol. 8 (2011) 30-41.

[3] Bergmann O, Bhardwaj RD, Bernard S, Zdunek S, Barnabé-Heider F, Walsh S, Zupicich J, Alkass K, Buchholz BA, Druid H. Evidence for cardiomyocyte renewal in humans. Science 324 (2009) 98-102.

[4] Ruschitzka F, Abraham WT, Singh JP, Bax JJ, Borer JS, Brugada J, Dickstein K, Ford I, Gorcsan III J, Gras D. Cardiac-resynchronization therapy in heart failure with a narrow qrs complex. N. Engl. J. Med. 369 (2013) 1395-1405.

[5] Hirt MN, Hansen A, Eschenhagen T. Cardiac tissue engineering: State of the art. Circ. Res. 114 (2014) 354-367.

[6] Carrier RL, Papadaki M, Rupnick M, Schoen FJ, Bursac N, Langer R, Freed LE, Vunjak-Novakovic G. Cardiac tissue engineering: Cell seeding, cultivation parameters, and tissue construct characterization. Biotechnol. Bioeng. 64 (1999) 580-589.

[7] Zhao G, Zhang X, Lu TJ, Xu F. Recent advances in electrospun nanofibrous scaffolds for cardiac tissue engineering. Adv. Funct. Mater. 25 (2015) 5726-5738.

[8] Shin SR, Zihlmann C, Akbari M, Assawes P, Cheung L, Zhang K, Manoharan V, Zhang YS, Yüksekkaya M, Wan Kt. Reduced graphene oxide ‐ gelma hybrid hydrogels as scaffolds for cardiac tissue engineering. Small 12 (2016) 3677-3689.

[9] Fleischer S, Shevach M, Feiner R, Dvir T. Coiled fiber scaffolds embedded with gold nanoparticles improve the performance of engineered cardiac tissues. Nanoscale 6 (2014) 9410-9414.

[10] Waters R, Pacelli S, Maloney R, Medhi I, Ahmed RP, Paul A. Stem cell secretome-rich nanoclay hydrogel: A dual action therapy for cardiovascular regeneration. Nanoscale 8 (2016) 7371-7376.

[11] KC P, Shah M, Liao J, Zhang G. Prevascularization of decellularized porcine myocardial slice for cardiac tissue engineering. ACS Appl. Mater. Inter. 9 (2016) 2196-2204.

[12] Qazi TH, Rai R, Dippold D, Roether JE, Schubert DW, Rosellini E, Barbani N, Boccaccini AR. Development and characterization of novel electrically conductive pani–pgs composites for cardiac tissue engineering applications. Acta Biomater. 10 (2014) 2434-2445.

[13] Spearman BS, Hodge AJ, Porter JL, Hardy JG, Davis ZD, Xu T, Zhang X, Schmidt CE, Hamilton MC, Lipke EA. Conductive interpenetrating networks of polypyrrole and polycaprolactone encourage electrophysiological development of cardiac cells. Acta Biomater. 28 (2015) 109-120.

[14] Ricotti L, Menciassi A. Bio-hybrid muscle cell-based actuators. Biomed. Microdevices 14 (2012) 987-998.

[15] Tanaka Y, Morishima K, Shimizu T, Kikuchi A, Yamato M, Okano T, Kitamori T. Demonstration of a pdms-based bio-microactuator using cultured cardiomyocytes to drive polymer micropillars. Lab Chip 6 (2006) 230-235.

[16] Chan V, Asada HH, Bashir R. Utilization and control of bioactuators across multiple length scales. Lab Chip 14 (2014) 653-670.

[17] Carlsen RW, Sitti M. Bio ‐ hybrid cell ‐ based actuators for microsystems. Small 10 (2014)

3831-3851.

[18] Ahadian S, Ramón-Azcón J, Chang H, Liang X, Kaji H, Shiku H, Nakajima K, Ramalingam M, Wu H, Matsue T. Electrically regulated differentiation of skeletal muscle cells on ultrathin graphene-based films. RSC Adv. 4 (2014) 9534-9541.

[19] Fujie T, Ahadian S, Liu H, Chang H, Ostrovidov S, Wu H, Bae H, Nakajima K, Kaji H, Khademhosseini A. Engineered nanomembranes for directing cellular organization toward flexible biodevices. Nano Lett. 13 (2013) 3185-3192.

[20] Raman R, Cvetkovic C, Uzel SG, Platt RJ, Sengupta P, Kamm RD, Bashir R. Optogenetic skeletal muscle-powered adaptive biological machines. Proc. Natl. Acad. Sci. U. S. A. 113 (2016) 3497-3502.

[21] Park SJ, Gazzola M, Park KS, Park S, Di Santo V, Blevins EL, Lind JU, Campbell PH, Dauth S, Capulli AK, Pasqualini FS, Ahn S, Cho A, Yuan H, Maoz BM, Vijaykumar R, Choi JW, Deisseroth K, Lauder GV, Mahadevan L, Parker KK. Phototactic guidance of a tissue-engineered soft-robotic ray. Science 353 (2016) 158-162.

[22] Yoon J, Eyster TW, Misra AC, Lahann J. Cardiomyocyte-driven actuation in biohybrid microcylinders. Adv. Mater. 27 (2015) 4509-4515.

[23] Vannozzi L, Ricotti L, Cianchetti M, Bearzi C, Gargioli C, Rizzi R, Dario P, Menciassi A. Self-assembly of polydimethylsiloxane structures from 2d to 3d for bio-hybrid actuation. Bioinspir. Biomim. 10 (2015) 056001.

[24] Fleischer S, Feiner R, Shapira A, Ji J, Sui X, Daniel Wagner H, Dvir T. Spring-like fibers for cardiac tissue engineering. Biomaterials 34 (2013) 8599-8606.

[25] Tallawi M, Rosellini E, Barbani N, Cascone MG, Rai R, Saint-Pierre G, Boccaccini AR. Strategies for the chemical and biological functionalization of scaffolds for cardiac tissue engineering: A review. J. R. Soc. Interface 12 (2015) 20150254.

[26] Chien KR, Domian IJ, Parker KK. Cardiogenesis and the complex biology of regenerative cardiovascular medicine. Science 322 (2008) 1494-1497.

[27] Kharaziha M, Nikkhah M, Shin SR, Annabi N, Masoumi N, Gaharwar AK, Camci-Unal G, Khademhosseini A. Pgs:Gelatin nanofibrous scaffolds with tunable mechanical and structural properties for engineering cardiac tissues. Biomaterials 34 (2013) 6355-6366.

[28] Orlova Y, Magome N, Liu L, Chen Y, Agladze K. Electrospun nanofibers as a tool for architecture

control in engineered cardiac tissue. Biomaterials 32 (2011) 5615-5624.

[29] Zong X, Bien H, Chung C-Y, Yin L, Fang D, Hsiao BS, Chu B, Entcheva E. Electrospun fine-textured scaffolds for heart tissue constructs. Biomaterials 26 (2005) 5330-5338.

[30] Liu Q, Tian S, Zhao C, Chen X, Lei I, Wang Z, Ma PX. Porous nanofibrous poly(l-lactic acid) scaffolds supporting cardiovascular progenitor cells for cardiac tissue engineering. Acta Biomater. 26 (2015) 105-114.

[31] Doshi J, Reneker DH. Electrospinning process and applications of electrospun fibers. Industry Applications Society Annual Meeting, 1993., Conference Record of the 1993 IEEE: IEEE; 1993. p. 1698-1703.

[32] Li D, Xia Y. Electrospinning of nanofibers: Reinventing the wheel? Adv. Mater. 16 (2004) 1151-1170.

[33] Reneker DH, Chun I. Nanometre diameter fibres of polymer, produced by electrospinning. Nanotechnology 7 (1996) 216.

[34] Teo W-E, Inai R, Ramakrishna S. Technological advances in electrospinning of nanofibers. Sci. Technol. Adv. Mater. 12 (2011) 013002.

[35] Chen J, Ge J, Guo B, Gao K, Ma PX. Nanofibrous polylactide composite scaffolds with electroactivity and sustained release capacity for tissue engineering. J. Mater. Chem. B 4 (2016) 2477-2485.

[36] Ma X, Ge J, Li Y, Guo B, Ma PX. Nanofibrous electroactive scaffolds from a chitosan-grafted-aniline tetramer by electrospinning for tissue engineering. RSC Adv. 4 (2014) 13652-13661.

[37] Li M, Guo Y, Wei Y, MacDiarmid AG, Lelkes PI. Electrospinning polyaniline-contained gelatin nanofibers for tissue engineering applications. Biomaterials 27 (2006) 2705-2715.

[38] Haraguchi Y, Shimizu T, Yamato M, Kikuchi A, Okano T. Electrical coupling of cardiomyocyte sheets occurs rapidly via functional gap junction formation. Biomaterials 27 (2006) 4765-4774.

[39] Noorman M, van der Heyden MA, van Veen TA, Cox MG, Hauer RN, de Bakker JM, van Rijen HV. Cardiac cell–cell junctions in health and disease: Electrical versus mechanical coupling. J. Mol. Cell. Cardiol. 47 (2009) 23-31.

[40] Hsiao CW, Bai MY, Chang Y, Chung MF, Lee TY, Wu CT, Maiti B, Liao ZX, Li RK, Sung HW. Electrical coupling of isolated cardiomyocyte clusters grown on aligned conductive nanofibrous

meshes for their synchronized beating. Biomaterials 34 (2013) 1063-1072.

[41] Kai D, Prabhakaran MP, Jin G, Ramakrishna S. Biocompatibility evaluation of electrically conductive nanofibrous scaffolds for cardiac tissue engineering. J. Mater. Chem. B 1 (2013) 2305-2314.

[42] Kharaziha M, Shin SR, Nikkhah M, Topkaya SN, Masoumi N, Annabi N, Dokmeci MR, Khademhosseini A. Tough and flexible cnt-polymeric hybrid scaffolds for engineering cardiac constructs. Biomaterials 35 (2014) 7346-7354.

[43] Guo B, Ma PX. Synthetic biodegradable functional polymers for tissue engineering: A brief review. Sci. China Chem. 57 (2014) 490-500.

[44] Jun I, Jeong S, Shin H. The stimulation of myoblast differentiation by electrically conductive sub-micron fibers. Biomaterials 30 (2009) 2038-2047.

[45] Guo B, Glavas L, Albertsson A-C. Biodegradable and electrically conducting polymers for biomedical applications. Prog. Polym. Sci. 38 (2013) 1263-1286.

[46] Li L, Ge J, Guo B, Ma PX. In situ forming biodegradable electroactive hydrogels. Polym. Chem. 5 (2014) 2880-2890.

[47] Zhao X, Li P, Guo B, Ma PX. Antibacterial and conductive injectable hydrogels based on quaternized chitosan-graft-polyaniline/oxidized dextran for tissue engineering. Acta Biomater. 26 (2015) 236-248.

[48] Wang L, Wu Y, Guo B, Ma PX. Nanofiber yarn/hydrogel core-shell scaffolds mimicking native skeletal muscle tissue for guiding 3d myoblast alignment, elongation, and differentiation. ACS Nano 9 (2015) 9167-9179.

[49] Chen J, Dong R, Ge J, Guo B, Ma PX. Biocompatible, biodegradable, and electroactive polyurethane-urea elastomers with tunable hydrophilicity for skeletal muscle tissue engineering. ACS Appl. Mater. Inter. 7 (2015) 28273-28285.

[50] Deng Z, Guo Y, Zhao X, Li L, Dong R, Guo B, Ma PX. Stretchable degradable and electroactive shape memory copolymers with tunable recovery temperature enhance myogenic differentiation. Acta Biomater. 46 (2016) 234-244.

[51] Xie M, Wang L, Guo B, Wang Z, Chen YE, Ma PX. Ductile electroactive biodegradable hyperbranched polylactide copolymers enhancing myoblast differentiation. Biomaterials 71 (2015) 158-167.

[52] Wu Y, Wang L, Guo B, Shao Y, Ma PX. Electroactive biodegradable polyurethane significantly enhanced schwann cells myelin gene expression and neurotrophin secretion for peripheral nerve tissue engineering. Biomaterials 87 (2016) 18-31.

[53] Qu J, Wang D, Wang H, Dong Y, Zhang F, Zuo B, Zhang H. Electrospun silk fibroin nanofibers in different diameters support neurite outgrowth and promote astrocyte migration. J. Biomed. Mater. Res. A 101(2013) 2667-2678.

[54] Xie M, Wang L, Ge J, Guo B, Ma PX. Strong electroactive biodegradable shape memory polymer networks based on star-shaped polylactide and aniline trimer for bone tissue engineering. ACS Appl. Mater. Inter. 7 (2015) 6772-6781.

[55] Guo B, Finne-Wistrand A, Albertsson A-C. Molecular architecture of electroactive and biodegradable copolymers composed of polylactide and carboxyl-capped aniline trimer. Biomacromolecules 11 (2010) 855-863.

[56] Guo B, Finne-Wistrand A, Albertsson A-C. Electroactive hydrophilic polylactide surface by covalent modification with tetraaniline. Macromolecules 45 (2011) 652-659.

[57] Zhao X, Wu H, Guo B, Dong R, Qiu Y, Ma PX. Antibacterial anti-oxidant electroactive injectable hydrogel as self-healing wound dressing with hemostasis and adhesiveness for cutaneous wound healing. Biomaterials 122 (2017) 34-47.

[58] Kim SB, Bae H, Cha JM, Moon SJ, Dokmeci MR, Cropek DM, Khademhosseini A. A cell-based biosensor for real-time detection of cardiotoxicity using lensfree imaging. Lab Chip 11 (2011) 1801-1807.

[59] Ostrovidov S, Shi X, Zhang L, Liang X, Kim SB, Fujie T, Ramalingam M, Chen M, Nakajima K, Al-Hazmi F, Bae H, Memic A, Khademhosseini A. Myotube formation on gelatin nanofibers - multi-walled carbon nanotubes hybrid scaffolds. Biomaterials 35 (2014) 6268-6277.

[60] Li L, Ge J, Wang L, Guo B, Ma PX. Electroactive nanofibrous biomimetic scaffolds by thermally induced phase separation. J. Mater. Chem. B 2 (2014) 6119-6130.

[61] Li L, Yu M, Ma PX, Guo B. Electroactive degradable copolymers enhancing osteogenic differentiation from bone marrow derived mesenchymal stem cells. J. Mater. Chem. B 4 (2016) 471-481.

[62] Niple J, Daigle J, Zaffanella L, Sullivan T, Kavet R. A portable meter for measuring low frequency currents in the human body. Bioelectromagnetics 25 (2004) 369-373.

[63] Pan HA, Hung YC, Sui YP, Huang GS. Topographic control of the growth and function of cardiomyoblast h9c2 cells using nanodot arrays. Biomaterials 33 (2012) 20-28.

[64] Ricotti L, Polini A, Genchi GG, Ciofani G, Iandolo D, Vazão H, Mattoli V, Ferreira L, Menciassi A, Pisignano D. Proliferation and skeletal myotube formation capability of c2c12 and h9c2 cells on isotropic and anisotropic electrospun nanofibrous phb scaffolds. Biomed. Mater. 7 (2012) 035010.

[65] Ricotti L, Polini A, Genchi GG, Ciofani G, Iandolo D, Mattoli V, Menciassi A, Dario P, Pisignano D. Nanostructured, highly aligned poly (hydroxy butyrate) electrospun fibers for differentiation of skeletal and cardiac muscle cells. Engineering in Medicine and Biology Society, EMBC, 2011 Annual International Conference of the IEEE: IEEE; 2011. p. 3597-3600.

[66] Jun I, Jeong S, Shin H. The stimulation of myoblast differentiation by electrically conductive sub-micron fibers. Biomaterials 30 (2009) 2038-2047.

[67] Skwarek-Maruszewska A, Hotulainen P, Mattila PK, Lappalainen P. Contractility-dependent actin dynamics in cardiomyocyte sarcomeres. J. Cell Sci. 122 (2009) 2119-2126.

[68] Schulz R, Heusch G. Connexin 43 and ischemic preconditioning. Cardiovasc. Res. 62 (2004) 335-344.

[69] Shin SR, Jung SM, Zalabany M, Kim K, Zorlutuna P, Kim SB, Nikkhah M, Khabiry M, Azize M, Kong J. Carbon-nanotube-embedded hydrogel sheets for engineering cardiac constructs and bioactuators. ACS nano 7 (2013) 2369-2380.

**Tables**

**Table 1.** Final weight ratio of PLA and PANI for the preparation of electrospun solution.

| Sample code | PLA (mg) | PANI (mg) | HFIP (mL) | PANI content (wt%) | CSA content (wt%) |
|---|---|---|---|---|---|
| PLA | 480 | 0 | 4 | 0 | 0 |
| PLA/PANI1.5 | 480 | 7.2 | 4 | 1.5 | 1.5 |
| PLA/PANI3 | 480 | 14.4 | 4 | 3 | 3 |

**Figure captions**

**Figure 1.** Preparation of PLA/PANI nanofibrous sheets via electrospinning. (a) Schematic diagrams displaying the electrospun processes for the fabrication of random conductive PLA/PANI nanofibrous sheets. (b) Optical images of PLA/PANI nanofibrous sheets with different PANI concentration including 0 wt%, 1.5 wt%, and 3 wt%, which were named as PLA (control group), PLA/PANI1.5, and PLA/PANI3, respectively. SEM images (c-e) and average diameters (f) of nanofibers in different PLA/PANI nanofibrous sheet groups. (g) Water contact angles of PLA/PANI nanofibrous sheets before and after immersing in medium for 24 h. (h) The cyclic voltammograms (CV) curves of the PLA/PANI3. (i) The electrical conductivity of PLA/PANI samples. *P<0.05.

**Figure 2.** The immunofluorescence staining of MYH2 (green) showed the myotube formation of H9c2 cells on PLA/PANI nanofibrous sheets after 6 days of differentiation (a). The quantitative results of myotube length (b), myotube number (c), myotube diameter (d), maturation index (e) and fusion index (f) were analyzed after 6 days of differentiation. *$P$<0.05.

**Figure 3.** The cell viability and morphology of cardiomyocytes on PLA/PANI nanofibrous sheets after culture for 2 days. Cardiomyocytes showed good cell viability on PLA/PANI nanofibrous sheets (c). The morphology of cardiomyocytes was visualized by the immunofluorescence staining of F-actin (green) (a). Insets are corresponding FFT images. White arrows showed the interconnected cells. Cellular orientation distribution derived from F-actin staining images were present (b). Aspect

ratio were also analyzed (d). *$P$<0.05.

**Figure 4.** Representative fluorescence images of CMs immunostained for sarcomeric α-actinin (green) and CX43 (red) on PLA (a), PLA/PANI1.5 (b) and PLA/PANI3 (c) nanofibrous sheets after culture for 8 days. The area fraction of α-actinin (d) and CX43 (e) were also analyzed. *$P$<0.05.

**Figure 5.** Beating characterization of cardiomyocytes on PLA/PANI nanofibrous sheets. (a) Beating frequency of CMs on nanofibrous sheets during 21 days of cultivation. Beating pattern of CMs on nanofibrous sheets at day 6 (b) and at day 21 (c).

**Figure 6.** Calcium transients of cardiomyocytes on PLA, PLA/PANI1.5 and PLA/PANI3 nanofibrous sheets. Three independent ROI were randomly selected in PLA(a), PLA/PANI1.5(b) and PLA/PANI3(c) groups. Line scanning across each ROI (d-f) groups captured spontaneous calcium transients; scale bar: 10 s. Dynamic changes of Ca2+ (F/F0) (g-i) also showed the normalized fluorescence intensity of each ROI.

**Figure 7.** PLA and PLA/PANI3 nanofibrous sheets formed 3D bioactuators with two different shapes (tubular and folding). (a) Schematic drawing of tubular and folding shaped bioactuators formed by CMs-laden nanofibrous sheets. (b) The gross images of two tubular bioactuators formed by CMs-laden PLA (i) and CMs-laden PLA/PANI3 (iv). Video images (ii, v) of two tubular bioactuators in the enclosed areas (red circles) from gross images. The displacement of tubular bioactuators formed by CMs-laden PLA (iii) and CMs-laden PLA/PANI3 (vi) was also represented.

(c) The gross images (i, iv), video images (ii, v) and displacement (iii, vi) of two folding bioactuators formed by CMs-laden PLA and CMs-laden PLA/PANI3.

**Figure 8.** Representative fluorescence images of CMs immunostained for CX43 (red) on tubular bioactuators formed by CMs-laden PLA (a) and CMs-laden PLA/PANI3 (b), and folding bioactuators formed by CMs-laden PLA (c) and CMs-laden PLA/PANI3 (d) after culture for 12 days.

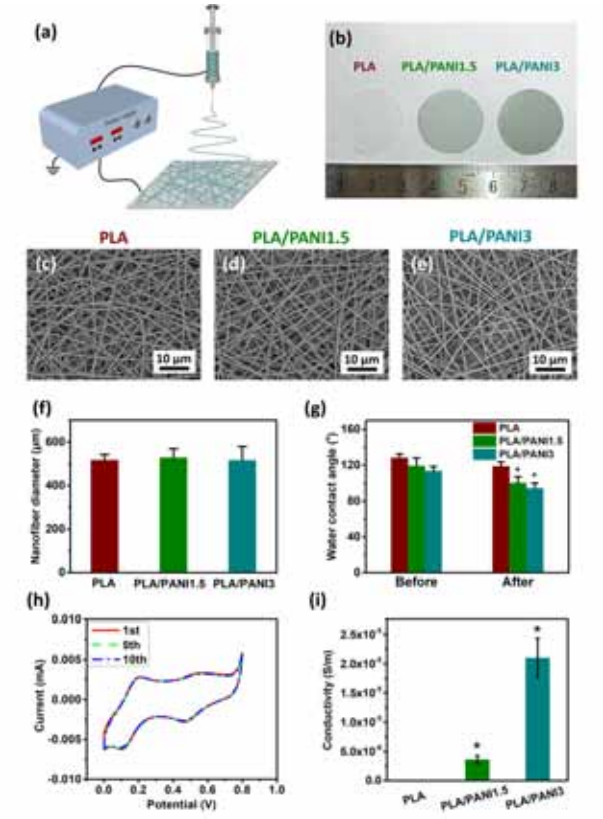

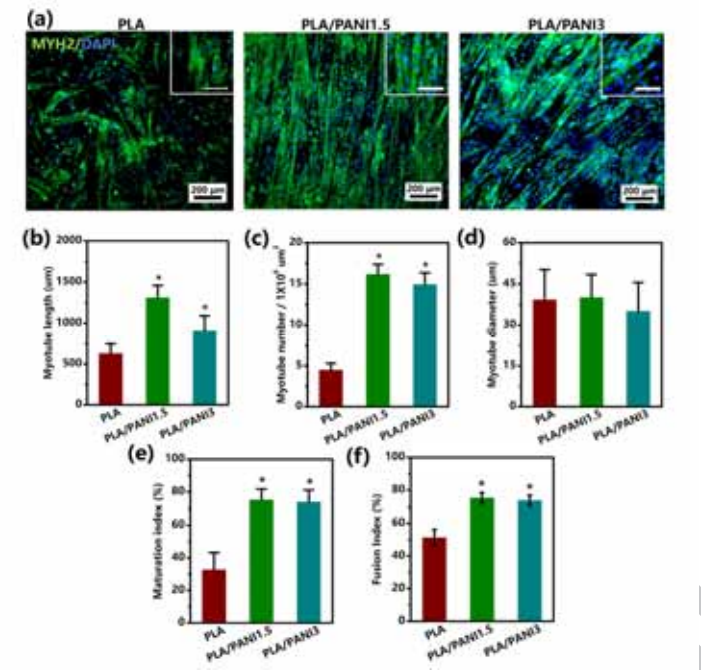

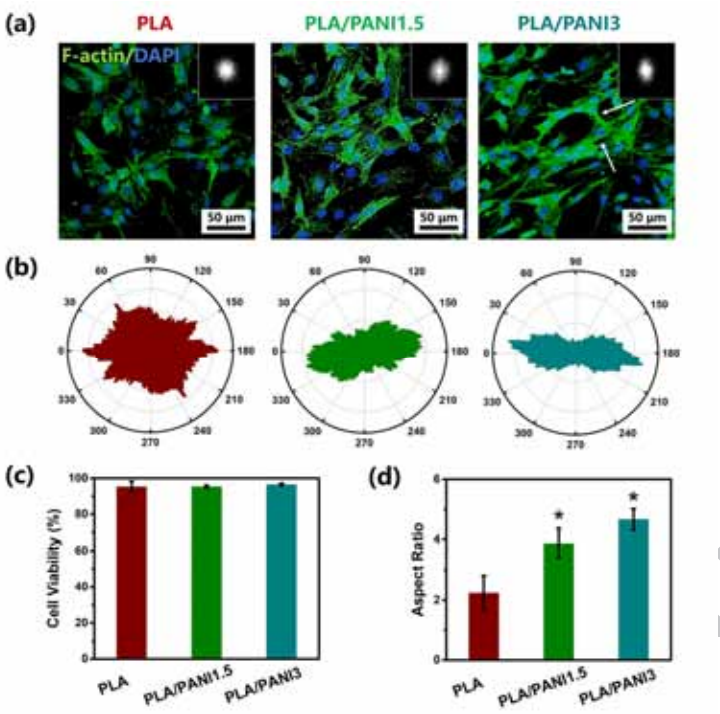

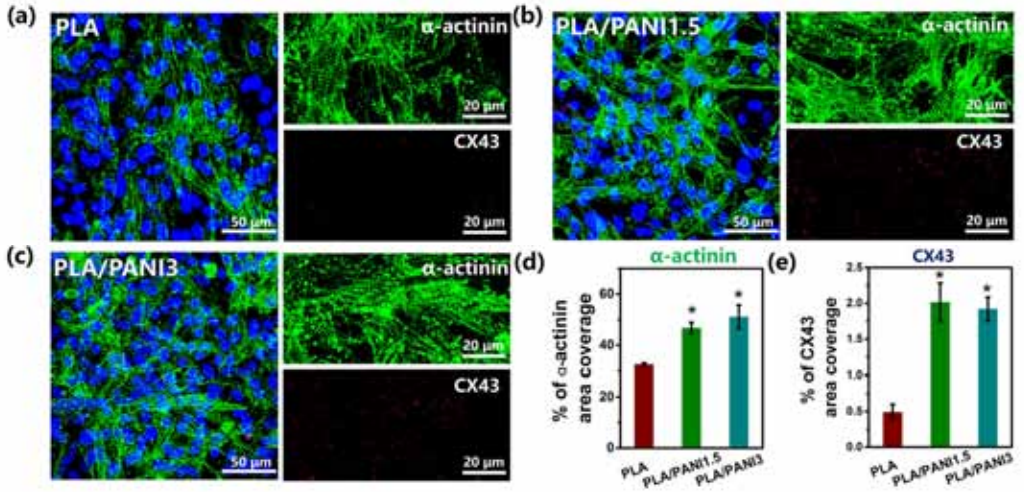

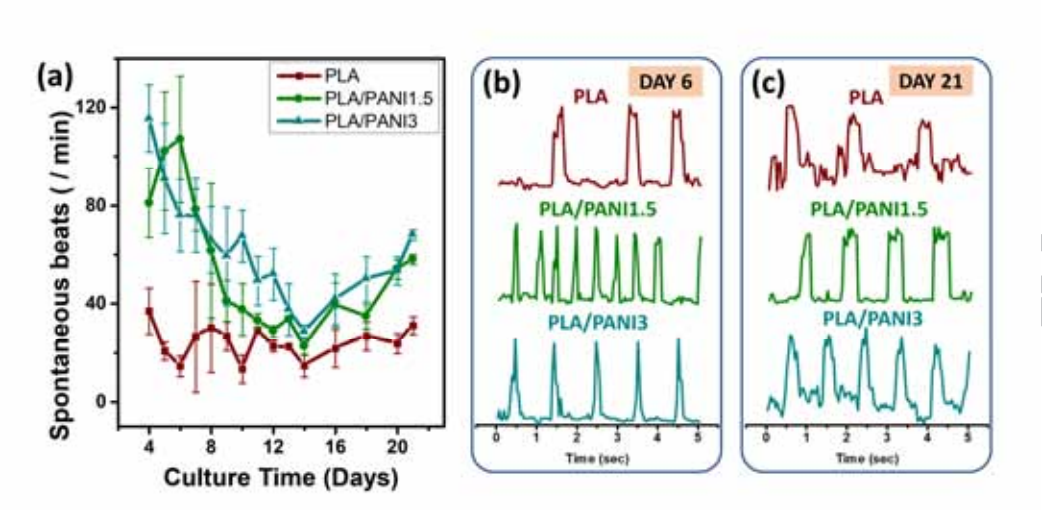

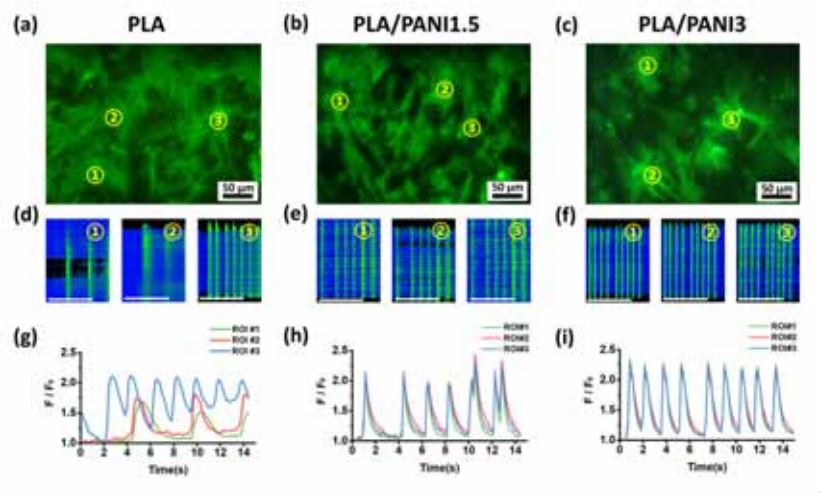

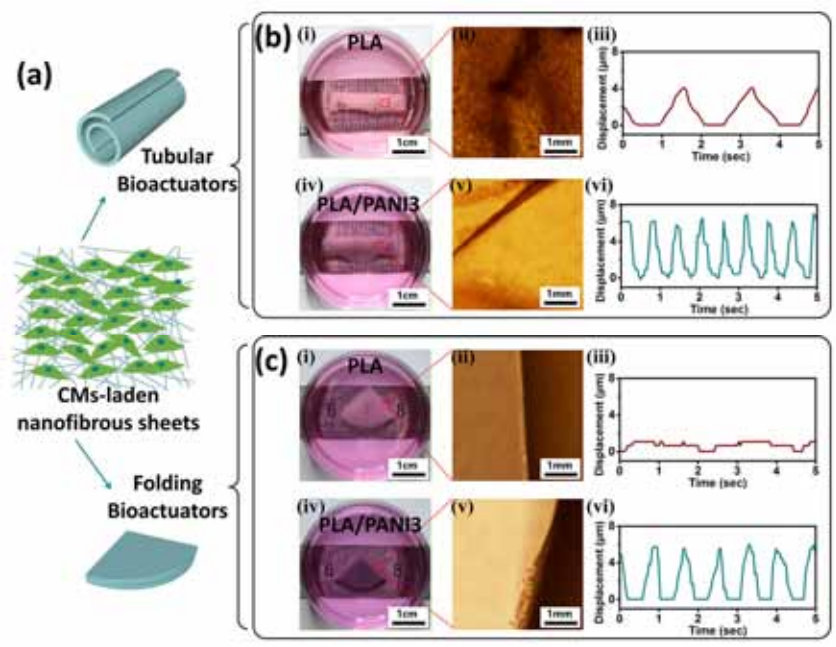

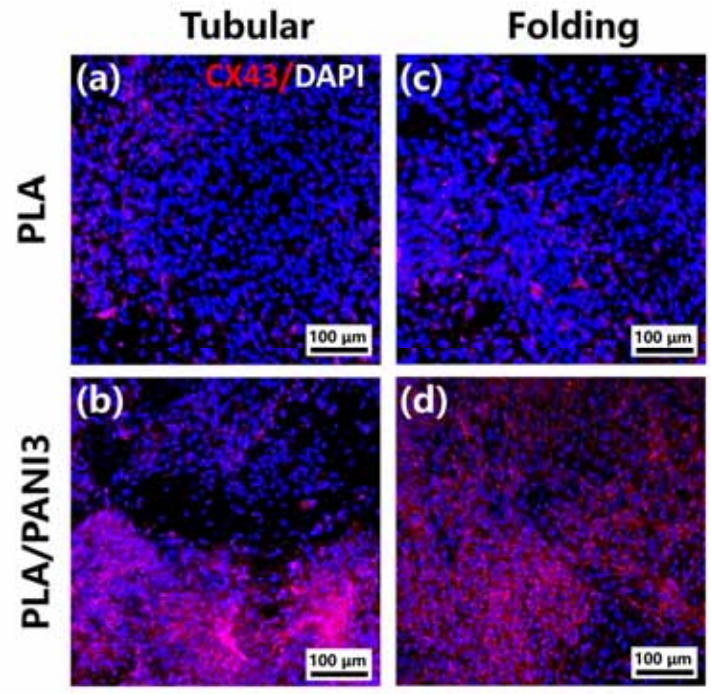

**Statement of Significance**

Cardiomyocytes-based bioactuators have been paid more attention due to their spontaneous motion by integrating cardiomyocytes into polymer structures, but developing suitable scaffolds for bioactuators remains challenging. Electrospun nanofibrous scaffolds have been widely used in cardiac tissue engineering because they can mimic the extracellular matrix of myocardium. Developing conductive nanofibrous scaffolds by electrospinning would be beneficial for cardiomyocytes-based bioactuators, but such scaffolds have been rarely reported. This work presented a conductive nanofibrous sheet based on polylactide and polyaniline via electrospinning with tunable conductivity. These conductive nanofibrous sheets performed the ability to enhance cardiomyocytes maturation and spontaneous beating, and further formed cardiomyocytes-based 3D bioactuators with tubular and folding shapes, which indicated their great potential in cardiac tissue engineering and bioactuators applications.